Idealized Glass Transitions under Pressure: Dynamics versus Thermodynamics

Th. Voigtmann

Institut für Materialphysik im Weltraum, Deutsches Zentrum für Luft- und Raumfahrt (DLR), 51170 Köln, Germany

(Received 18 January 2008; revised manuscript received 14 July 2008; published 28 August 2008)

The interplay of slow dynamics and thermodynamic features of dense liquids is studied by examining how the glass transition changes depending on the presence or absence of Lennard-Jones-like attractions. Quite different thermodynamic behavior leaves the dynamics unchanged, with important consequences for high-pressure experiments on glassy liquids. Numerical results are obtained within mode-coupling theory (MCT), but the qualitative features are argued to hold more generally. A simple square-well model can be used to explain generic features found in experiment.

DOI: 10.1103/PhysRevLett.101.095701 PACS numbers: 64.70.Q−, 62.50.−p

The quest for identifying the physical mechanism behind the dynamical transformation of a liquid into an amorphous solid, the glass transition, has prompted many studies aiming to disentangle the dominant control variables involved. Slow dynamics connected with the transition is recognized to be universal, but its connection to the underlying liquid structure is highly debated [1–5]. Some argue in terms of a density effect called free volume; others attribute the main physics to energetic interactions and thermally activated processes.

Experiments changing both temperature T and pressure P are emerging to resolve such issues, but have brought contradictory results. Some find that temperature dominates glassy dynamics by far [6–9]; some find that it does not [10–12]. Others find both variables to exert equal influence [13–22], some with temperature [23–27], some with density ϱ being more relevant [28–31]. The difficulty of obtaining data over wide pressure ranges might be impeding: few studies, pioneered only in the 1990's [28,32], go beyond 1 GPa.

Here we propose that to resolve the apparent contradictions, one needs to *separate* nonuniversal thermodynamic aspects, i.e., the equation of state (EOS) of the system, from universal dynamical features, viz., the slow relaxation. We show how the presence or absence of attractive interactions affects the glass transition, and how this emerges in different pairs of variables linked by the EOS: (ϱ, T) (preferred by theory) vs (P, T) (more amenable to experiments), yielding a transition that appears "temperature-driven" in the latter.

The Lennard-Jones (LJ) potential serves as a realistic interaction model: $V_{\mathrm{LJ}}(r) = 4\epsilon[(r/\sigma)^{-12} - (r/\sigma)^{-6}]$, with dimensionless parameters $\varrho^* = \varrho\sigma^3$, $T^* = 1/(\beta\epsilon)$, $P^* = P\sigma^3/\epsilon$; $\beta = 1/(k_B T)$ with Boltzmann's constant k_B. To study relative effects of entropy and energy, we compare the LJ glass transition with that of its purely repulsive (LJR) counterpart, $V_{\mathrm{LJR}}(r) = V_{\mathrm{LJ}}(r) + \epsilon \geq 0$ for $r \leq 2^{1/6}\sigma$, $V_{\mathrm{LJR}}(r) = 0$ else. For the transition lines, mode-coupling theory (MCT) [33,34] provides a reasonable qualitative description. Its transition temperature T_c is systematically above the experimental (calorimetric) one, T_g, but nevertheless serves as a good indicator for the change from high-T liquidlike dynamics to a low-T glass-like one [35,36]. In MCT, T_c is the point where the glass form factor $f(q)$, measuring an elastic response to the scattering spectrum, jumps discontinuously (usually from zero to a finite value) due to a bifurcation in [34]

$$\frac{f(q)}{1-f(q)} = \frac{\varrho S(q)}{2q^4}\int \frac{d^3k}{(2\pi)^3}\mathcal{V}(\boldsymbol{q},\boldsymbol{k})f(k)f(p), \quad (1)$$

$\mathcal{V}(\boldsymbol{q},\boldsymbol{k}) = S(k)S(p)[q^2 - \boldsymbol{q}\cdot\boldsymbol{k}/S(k) - \boldsymbol{q}\cdot\boldsymbol{p}/S(p)]^2/\varrho^2$, with $q = |\boldsymbol{q}|$, $p = |\boldsymbol{q}-\boldsymbol{k}|$. Equation (1) is solved by an iteration scheme [37]. The interaction potential $V(r)$ and temperature T enter only through the static structure factor $S(q)$, obtained in the hypernetted-chain (HNC) approximation [38,39]. $S(q=0)$ determines the pressure through the equation of state (EOS),

$$\beta P = \int_0^{\varrho} d\hat{\varrho}\, S(q=0,\hat{\varrho},T)^{-1}, \quad (2)$$

integrated numerically for the LJ and LJR systems. We have checked that the quantitative error of the HNC closure does not influence our results qualitatively.

The MCT glass transitions for the two systems are almost identical, i.e., they depend very little on the presence or absence of attractive interactions. As shown in Fig. 1, the lines in a T-ϱ diagram coincide on the scale of the figure. In fact, most of the change in $T_c(\varrho)$ can be understood from the soft-sphere limit: for $T \to \infty$, $V_{\mathrm{LJ}(R)}(r) \sim \epsilon(r/\sigma)^{-n}$, $n = 12$, and the only control parameter is an effective packing fraction, $\varphi_{\mathrm{eff}} = (\pi/6)\varrho\sigma_{\mathrm{eff}}^3$, where $\sigma_{\mathrm{eff}}^3 = \sigma^3 T^{*-3/n}$ accounts for the soft core. The dash-dotted line in Fig. 1 corresponds to this soft-sphere glass transition, $\varrho_c \propto T_c^{-3/n}$, where Eq. (1) yields $\varphi_{\mathrm{eff}}^c \approx 0.564$. It clearly shows the same qualitative behavior as the $T_c(\varrho)$ lines for the full LJ system. Molecular-dynamics simulation data on the LJ glass transition collected in Ref. [40] and estimates from the energy-landscape calculations of Ref. [41] are reproduced in Fig. 1 as triangles. They agree

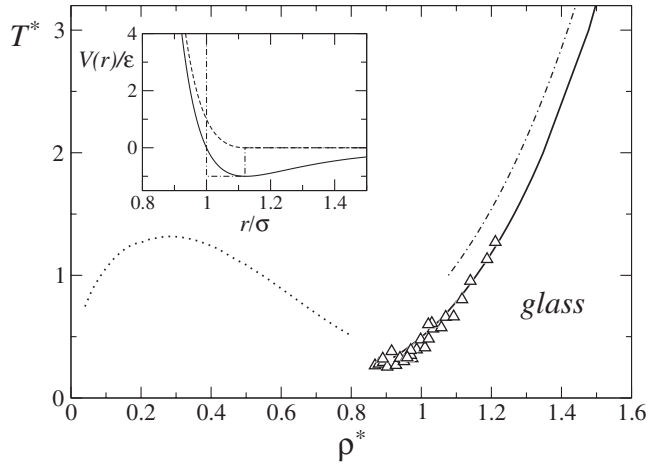

FIG. 1. Glass-transition lines for the Lennard-Jones system with and without attractions: MCT results for both coincide (solid line). Triangles are glass-transition points from simulations [40,41]. Dash-dotted line: soft-sphere asymptote, $T_c^*(\varrho) \approx (\pi/6\varphi_{\rm eff}^c)^4\varrho^4$, $\varphi_{\rm eff}^c = 0.564$. The dotted line indicates a gas-liquid spinodal. Inset: LJ (solid line), LJR (dashed), and square-well ($\delta = 0.12$; dash-dotted) potentials.

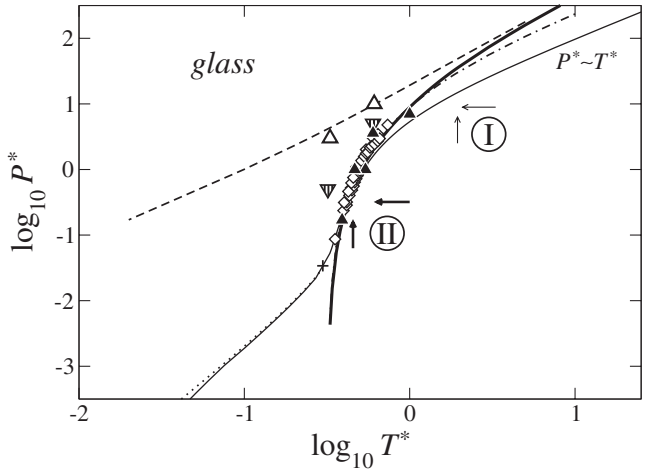

FIG. 2. Lennard-Jones glass transitions with (thick line) and without (dashed) attractions in a pressure-vs-temperature representation, from MCT. Triangles: simulation data from Refs. [40,45] (filled: LJ; open: purely repulsive; inverted: truncated LJ). Dash-dotted line: LJ transition as $P_{\rm eff}^* = P^*T^{-1/4}$. Thin solid line: square-well model transition ($\delta = 0.12$, shifted as $T^* \mapsto 1.5T^*$); dotted: square-well model spinodal with critical point (cross). Diamonds: experimental data for glycerol (Refs. [28,49]), see text. Arrows indicate isobars and isotherms used in Fig. 3.

with our results reasonably well, considering the different definitions of the glass-transition point used in these works.

Attractions are crucial for the thermodynamics: they introduce a gas-liquid spinodal, whose estimate is shown in Fig. 1 (dotted line). The compressibility diverges smoothly there, $1/S(q=0) \to 0$. Hence, the resulting $P(\varrho, T)$ values in the liquid, Eq. (2), are significantly lower with than without attractions, i.e., for $T < T_{\rm cr}$ and $\varrho > \varrho_{\rm cr}$, where $(\varrho_{\rm cr}, T_{\rm cr})$ is the gas-liquid critical point. This even holds for approximations that fail to predict the spinodal correctly (such as HNC) [42]. In other words, LJ-like attractions in high-density liquids simply affect the pressure: the contributions of all particles add up to a flat background that does not influence the forces [43], nor the (glassy) dynamics.

Figure 2 demonstrates the marked effect the spinodal has on the glass-transition line in the P-T diagram: nearly indistinguishable in the T-ϱ diagram, Fig. 1, the transition lines with (LJ) and without (LJR) attraction (thick solid and dashed lines) now appear qualitatively different. The LJ $\log P_c$-versus-$\log T$ line has a steep part not present in the LJR line at $\log_{10}T^* < 0.1$, corresponding to $T^* < T_{\rm cr}^* \approx 1.4$. It stops at the spinodal, restricting the glassy regime to densities $\varrho > \varrho_{\rm cr}$ [44]. Simulation data from Refs. [40,45] (triangles in Fig. 2) scatter between the LJ and LJR lines since different truncations of the potential were used, yielding different equations of state. The data from Ref. [40] for several truncations collapse to a single curve in Fig. 1 within error bars, confirming our finding.

This is easily understood within MCT: the glass transition in dense systems is driven by nearest-neighbor interactions (the cage effect), i.e., by features of the structure factor $S(q)$ at $q \approx 2\pi/\sigma$. But the attractions affect only $S(q \to 0)$ [46]; a region strongly suppressed in the MCT integral, Eq. (1). Merely the transformation $\varrho \mapsto P$ is dominated by $q \to 0$ effects.

Since this transformation in general relies on cumbersome numerical calculations, we simplify matters by introducing a square-well (SW) potential as a "cartoon" of the LJ model, showing first that the qualitative features discussed above are preserved. The SW model consists of a hard-sphere core and an attraction of relative width δ: $V_{\rm SW}(r) = -\epsilon$ for $1 < r/\sigma < 1 + \delta$. Here, a mean-spherical approximation (MSA) for $S(q)$ [47] allows the integration of Eq. (2) analytically. The MCT line for $\delta = 0.12$ [37] is shown in Fig. 2, rescaled as $T^* \mapsto 1.5T^*$ to account for the different $S(q)$ approximation inducing a shift in T scale [47].

We identify two generic regimes for both the LJ and the square-well lines: $T^* \to \infty$ is the hard-sphere limit where the glass transition occurs along an isochore $P_c \sim k_BT$; this limit is approached for $T^* \gtrsim 1$ (regime I). It is also present in the LJ system, provided one corrects for soft-core effects, $P_{\rm eff}^* = P^*T^{-3/n}$, as the dash-dotted line shows. For $0.1 \lesssim T^* \lesssim 1$ the steep $\log P_c^*$-versus-$\log T^*$ line discussed above is found in both models (regime II). Its position along the T^* axis scales with the gas-liquid critical temperature ($T_{\rm cr}^* \sim \delta$ for the MSA-SW). For $T^* \to 0$, the SW model shows a low-density regime corresponding to $\varrho < \varrho_{\rm cr}$ (a cross marks the point where $\varrho_c = \varrho_{\rm cr}$), where the dynamics itself strongly depends on the potential depth ϵ.

This attraction-driven regime may be connected with colloidal gelation and is absent in the Lennard-Jones model and in common molecular glasses. Relevant for typical glass formers at MPa pressures is regime II, as pointed out recently [48]: experiments reveal steep $P(T_g)$ curves that are incompatible with the hard-sphere-like regime I. Diamond symbols in Fig. 2 exemplify this for glycerol: experimental $T_g(P)$ data from Refs. [28,49] was mapped according to $\epsilon/k_B = 500$ K and $\epsilon/\sigma^3 = 2.5$ GPa, just to demonstrate qualitative agreement (and absorbing the quantitative difference between T_g and T_c in the mapping).

Our discussion of glass-transition lines has direct implications for dynamical quantities, as the latter are expected to depend strongly on the distance to the transition. For example, a "thermodynamic scaling" has been observed for many glass formers, involving $\varrho T^{-\gamma}$ as a scaling variable [8,31,50–52] or density-dependent interaction energy [9]. γ is an empirical, effective exponent: even in the LJ system, $\gamma \neq 1/4 = 3/n$ [53]. In agreement with this, we find that the LJ transition line can be well fitted for all $T^* < 3$ by $\varrho_c^*(T) \propto T^\gamma$, where $\gamma = 0.15 \ldots 0.23$. Partly, this merely mirrors that effective power laws can be used to fit the potential in the respective $V(r)/\epsilon \approx T^*$ range. If attractions are present, the effective γ also depends on their details, as strikingly demonstrated by the SW system, where we do not find the $\gamma \to 0$ expected from the $n \to \infty$ hard-sphere limit.

One can characterize the relative effects of temperature and pressure on the glass transition by monitoring the viscosity η along isotherms and isobars, using density as a parameter. Experiments [6,10,11,17–29] usually find stronger variation along an isobar (varying T) than along an isotherm (varying P). This is a natural consequence of our scenario, evidenced in Fig. 3 by the viscosity η^* in SW units, calculated from the standard Green-Kubo expression in the MCT approximation [33]. Consider regime II: changing T along the $P^* = 0.316$ isobar (solid line) corresponds to a more direct approach to the glass-transition line as compared to changing P along the $T^* = 0.3$ isotherm (dashed); cf. the thick arrows in Fig. 2. Clearly, η^* diverges over a smaller density interval along the isobar. Agreement with experiment is semiquantitative, as the symbols, reproduced from Ref. [17] demonstrate. Only in regime I (inset of Fig. 3; thin arrows in Fig. 2) do P and T exert equal influence. Not all transition points are equal: MCT predicts nonuniversal amplitudes and shapes for relaxation spectra that change along the transition line, invalidating a "temperature-pressure" superposition principle. But changes are small enough to make it appear to work, explaining why some experiments find it [12–15,24,49], some with restrictions [27,54–56], some not at all [25,57].

Temperature and density effects are often quantified by a ratio of activation energy and enthalpy [6,31,58], $E_V/H_P = (\partial \log\tau/\partial T^{-1})_V/(\partial \log\tau/\partial T^{-1})_P$, trivially related to $E = (\partial\varrho/\partial T)_\tau(\partial T/\partial\varrho)_P$. Large $|E|$ signify a temperature-driven transition, small $|E|$ a density-driven one. E consists of a glass-transition part, and a purely EOS-driven one. According to Fig. 1, the isokinetic term $r = (\partial\varrho/\partial T)_\tau$ does not depend on LJ-like attraction; the EOS term $t = (\partial T/\partial\varrho)_P$, however, changes. Estimating the latter through the SW-MSA expression, we find that t *decreases* in the vicinity of the spinodal: $|E|$ increases with P, indicating a growing influence of temperature at higher pressures. Such trends have been found and argued to be at odds with the expectation that the transition becomes hard-sphere like at high P [9]. According to our model, they are dominantly thermodynamic effects.

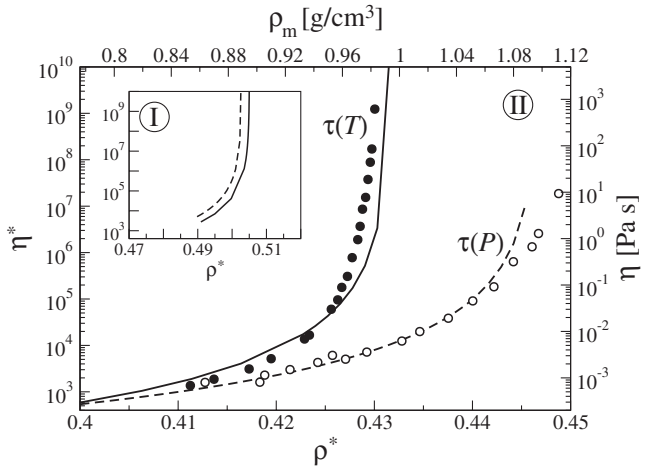

FIG. 3. Typical relaxation times τ as functions of density: MCT results for the SW system ($\delta = 0.12$; bottom and left axes), along the isobar $P^* = 0.316$ (solid line) and the isotherm $T^* = 0.3$ (dashed), marked by thick arrows in Fig. 2. Symbols (upper/right axes) are viscosity data for isopropylbenzene [17] for the isobar $P = 0.1$ MPa (filled) and the isotherm $T = 293$ K (open). Inset: MCT results for $P^* = 8.91$ (solid line) and $T^* = 0.775$ (dashed line); thin arrows in Fig. 2.

A similar conclusion holds for the pressure dependence of "fragility" used to classify how quickly relaxation times diverge. Recent work debated its relation to $q \to 0$ quantities such as elastic constants, the above energy-enthalpy ratio or the exponent γ [1–5,56,59]. If true, MCT predicts a pressure dependent fragility that is a nonuniversal feature of $S(q \to 0)$, less so of the glassy dynamics [60]. This may hint towards why, e.g., hydrogen bonds drastically change the high-pressure behavior regarding fragility and thermodynamic scaling [59].

In conclusion, MCT glass-transition lines for the Lennard-Jones system and for the same system truncated to be purely repulsive are nearly identical in a ϱ-T plot, Fig. 1. Yet, they appear quite different in a P-T diagram, Fig. 2. The difference can be understood as unrelated to the glass-transition mechanism itself, but to a difference in thermodynamic behavior only. If one accepts that the glass transition is a primarily dynamic phenomenon, it will not

be altered by sufficiently long-ranged, LJ-like, attractions. However, the equation of state, determining the pressure of the system, will change. The P_c-versus-T curve hence has two regimes if attractions are present. In the very high-pressure regime I, it is essentially a density-driven fluid-glass transition: $P_c \propto T$, after correcting for soft-core effects. In regime II, identified as the experimentally relevant one, the existence of a gas-liquid spinodal leads to $T_c(P)$ curves with a much weaker P dependence: this could be called a temperature-driven liquid-glass transition; but temperature driven is not equivalent to ''attraction dominated.'' Key qualitative features can be understood within the square-well system as a better tractable model. Discussing the glass transition in terms of ''temperature vs pressure'' might obscure the physics responsible for it, focusing too much on different thermodynamics of different glass formers. For example, a composition change in metallic glass formers greatly changes the thermodynamics, little affecting the slow dynamics [61]. Experiments probing pressures $P \gg 1$ GPa seem desirable to test the picture proposed here.

I thank M. Sperl, M. E. Cates, W. C. K. Poon, A. Meyer, and W. Götze for discussions and EPSRC (GR/S10377) and DFG (Vo-1270/1) for funding.

[1] K. Ito, C. T. Moynihan, and C. A. Angell, Nature (London) **398**, 492 (1999).
[2] S. Sastry, Nature (London) **409**, 164 (2001).
[3] P. Bordat *et al.*, Phys. Rev. Lett. **93**, 105502 (2004).
[4] V. N. Novikov and A. P. Sokolov, Nature (London) **431**, 961 (2004).
[5] S. N. Yannopoulos and G. P. Johari, Nature (London) **442**, E7 (2006).
[6] M. L. Ferrer *et al.*, J. Chem. Phys. **109**, 8010 (1998).
[7] S. Hensel-Bielowka *et al.*, J. Phys. Chem. B **106**, 12 459 (2002).
[8] C. Dreyfus *et al.*, Phys. Rev. E **68**, 011204 (2003).
[9] G. Tarjus *et al.*, J. Chem. Phys. **120**, 6135 (2004).
[10] M. Paluch, C. M. Roland, and A. Best, J. Chem. Phys. **117**, 1188 (2002).
[11] M. Paluch, R. Casalini, and C. M. Roland, Phys. Rev. B **66**, 092202 (2002).
[12] A. Barbieri *et al.*, J. Chem. Phys. **120**, 437 (2004).
[13] S. Corezzi *et al.*, Phys. Rev. E **60**, 4444 (1999).
[14] L. Comez *et al.*, Phys. Rev. E **66**, 032501 (2002).
[15] R. Casalini *et al.*, J. Chem. Phys. **117**, 4901 (2002).
[16] M. Paluch, S. Hensel-Bielówka, and J. Zio lo, Phys. Rev. E **61**, 526 (2000).
[17] G. Li *et al.*, Phys. Rev. Lett. **74**, 2280 (1995).
[18] M. Paluch *et al.*, J. Chem. Phys. **117**, 7624 (2002).
[19] M. Paluch *et al.*, J. Chem. Phys. **118**, 3177 (2003).
[20] C. M. Roland and R. Casalini, Macromolecules **36**, 1361 (2003).
[21] K. Mpoukouvalas and G. Floudas, Phys. Rev. E **68**, 031801 (2003).
[22] M. Paluch *et al.*, Phys. Rev. E **68**, 031802 (2003).
[23] H. Leyser *et al.*, Phys. Rev. E **51**, 5899 (1995).
[24] C. M. Roland *et al.*, Macromolecules **36**, 4954 (2003).
[25] R. Casalini and C. M. Roland, J. Chem. Phys. **119**, 4052 (2003).
[26] R. Casalini and C. M. Roland, J. Chem. Phys. **119**, 11 951 (2003).
[27] P. Papadopoulos *et al.*, Macromolecules **37**, 8116 (2004).
[28] R. L. Cook *et al.*, J. Chem. Phys. **100**, 5178 (1994).
[29] M. Paluch *et al.*, J. Chem. Phys. **118**, 4578 (2003).
[30] A. Barbieri, G. Gorini, and D. Leporini, Phys. Rev. E **69**, 061509 (2004).
[31] C. M. Roland *et al.*, J. Chem. Phys. **120**, 10 640 (2004).
[32] R. L. Cook, C. A. Herbst, and H. E. King, Jr., J. Phys. Chem. **97**, 2355 (1993).
[33] U. Bengtzelius, W. Götze, and A. Sjölander, J. Phys. C **17**, 5915 (1984).
[34] W. Götze, in *Liquids, Freezing and Glass Transition*, edited by J. P. Hansen, D. Levesque, and J. Zinn-Justin (North Holland, Amsterdam, 1991), p. 287.
[35] V. N. Novikov and A. P. Sokolov, Phys. Rev. E **67**, 031507 (2003).
[36] A. Meyer, Phys. Rev. B **66**, 134205 (2002).
[37] $M = 200$ q points with cutoff $Q\sigma = 80$; for the square-well model, $M = 600$ and $Q\sigma = 240$.
[38] J.-P. Hansen and I. R. McDonald, *Theory of Simple Liquids* (Academic Press, London, 1986), 2nd ed.
[39] S. Labik, A. Malijevsky, and P. Vonka, Mol. Phys. **56**, 709 (1985).
[40] U. Bengtzelius, Phys. Rev. A **33**, 3433 (1986).
[41] R. di Leonardo *et al.*, Phys. Rev. Lett. **84**, 6054 (2000).
[42] L. Belloni, J. Chem. Phys. **98**, 8080 (1993).
[43] B. Widom, Science **157**, 375 (1967).
[44] S. S. Ashwin, G. I. Menon, and S. Sastry, Europhys. Lett. **75**, 922 (2006).
[45] W. J. Ma and S. K. Lai, Physica (Amsterdam) **233B**, 221 (1997).
[46] J. D. Weeks, D. Chandler, and H. C. Andersen, J. Chem. Phys. **54**, 5237 (1971).
[47] K. Dawson *et al.*, Phys. Rev. E **63**, 011401 (2000); M. Sperl, Diploma thesis, TU Munich (2000).
[48] Th. Voigtmann and W. C. K. Poon, J. Phys. Condens. Matter **18**, L465 (2006).
[49] M. Paluch *et al.*, J. Chem. Phys. **116**, 9839 (2002).
[50] R. Casalini and C. M. Roland, Phys. Rev. E **69**, 062501 (2004).
[51] S. Pawlus *et al.*, Phys. Rev. E **70**, 061501 (2004).
[52] C. M. Roland and R. Casalini, J. Non-Cryst. Solids **351**, 2581 (2005).
[53] D. Coslovich and D. M. Roland, J. Phys. Chem. B **112**, 1329 (2008).
[54] S. Hensel-Bielowka *et al.*, Phys. Rev. E **69**, 050501 (2004).
[55] M. Sekula *et al.*, J. Phys. Chem. B **108**, 4997 (2004).
[56] K. Niss *et al.*, J. Phys. Condens. Matter **19**, 076102 (2007).
[57] A. Patkowski, M. M. Lopez, and E. W. Fischer, J. Chem. Phys. **119**, 1579 (2003).
[58] G. Williams, Trans. Faraday Soc. **60**, 1556 (1964).
[59] C. M. Roland *et al.*, Phys. Rev. B **77**, 012201 (2008).
[60] Th. Voigtmann, J. Non-Cryst. Solids **352**, 4826 (2006).
[61] S. Mavila Chathoth *et al.*, Appl. Phys. Lett. **85**, 4881 (2004).